

Transport Enhancing Features of ETG Turbulence

N. Joiner and A. Hirose

Plasma Physics Laboratory, University of Saskatchewan, Saskatoon, Canada

Email:nathan.joiner@usask.ca

Abstract. Electron Temperature Gradient driven (ETG) modes have been proposed as a source of anomalous electron thermal losses in tokamaks. It is widely acknowledged that the electrostatic potential in ETG turbulence can develop into radially elongated structures known as streamers. Understanding the conditions that permit streamers to produce experimentally significant transport is a topic of great interest. Analysis of the ETG mode at long wavelengths where both the ions and electrons are adiabatic ($k_{\perp}\rho_i \gg 1$ and $\omega \ll k_{\parallel}v_{te}$) show that the ETG mode is inherently electromagnetic. Mixing length estimates of the thermal transport coefficient in this regime peak at c/ω_{pe} scales, providing a possible β dependence of the resulting transport. Preliminary nonlinear flux-tube simulations of the electromagnetic ETG mode produce large transport from the magnetic nonlinearity, while streamers in the electrostatic potential are still formed. Nonlinear simulations of ETG turbulence using GS2, show a dramatic decrease in transport if trapped electrons are removed from the calculation. This is shown to be due to stabilisation of the linear modes.

1. Introduction

There are regimes in tokamak experiments where the ion thermal transport is reported to be at the neo-classical level while the electron thermal transport is anomalous, such as Internal Transport Barriers (ITBs) and Spherical Tokamaks (STs). Simulations of Electron Temperature Gradient driven (ETG) micro-turbulence have been shown to produce an electron thermal diffusivity relevant to experimental values [1]. Therefore, understanding when ETG turbulence can produce thermal transport that exceeds gyro-Bohm estimates is important for predicting and controlling electron heat losses.

Although the thermal transport in ETG turbulence is dominated by electrostatic fluctuations, a dependence on β ($\delta B \propto \beta$) the ratio of plasma pressure to magnetic pressure has been observed in nonlinear simulations [2, 3]. When δB_{\parallel} is neglected the effect of the parallel magnetic vector potential on the linear ETG mode is generally negligible [3, 4].

Kim and Horton [5] noted that the electromagnetic effect on the linear mode would be largest when perpendicular wavelengths are comparable to the collisionless skin depth ($ck_{\perp}/\omega_{pe} \sim 1$ where $\omega_{pe} = \sqrt{(m_e/4\pi n_0 e^2)}$). Numerical solution of the full local dispersion relation shows that finite β is required to destabilise ETG modes with low values of k_y . The analysis presented in [5] does not capture this.

In the limit $\omega \gg k_{\parallel}v_{te}$, if we assume a strong toroidal character so that $\omega \sim \omega_D = 2\omega_* L_n/R = 2k_y \rho_e v_{te}/R$ and $k_{\parallel} \sim 1/qR$, then $k_y \rho_e \gg 1/2q$ must be satisfied. For typical values of q and β this does not capture skin depth sized ETG modes, and so we see that $\omega \ll k_{\parallel}v_{te}$ is more appropriate for toroidal ETG modes with $k_{\perp} \ll 1$.

In section 2 we present an analysis in the limit $\omega \ll k_{\parallel}v_{te}$ that predicts an electromagnetic ETG mode for wavenumbers $k_{\perp}c/\omega_{pe} \lesssim 1$. This mode differs from

previous electromagnetic ETG calculations in that a magnetic perturbation is essential. This skin-depth sized electromagnetic ETG mode is found to be unstable for values of η_e below the usual critical value for large enough β . Preliminary nonlinear calculations using the flux-tube code GS2 [1, 6] in this regime, give large transport dominated by magnetic flutter.

The presence of trapped electrons in ETG turbulence has been found to have an effect on the resulting thermal transport [7]. In section 3 we find that the linear growth rates are significantly altered when trapped particles are removed from the calculation, offering some explanation to the large differences in transport observed in [7]. Since the growth rates are insensitive to $\epsilon = r/R$ when trapped particles are retained, it is likely that large pitch angles are important rather than the bounce motion of trapped particles having any significance.

2. Skin-depth sized electromagnetic ETG modes

In the limit $\omega \ll k_{\parallel}v_{te}$ and $k_{\perp}^2 \ll 1$ the equation for the perturbed electron density is,

$$n_e = -\phi - \frac{(\omega - \omega_*)A_{\parallel}}{k_{\parallel}} \quad (1)$$

where density is normalised by n_0 , ϕ and A_{\parallel} are normalised to $|e|/T_e$ and $|e|c/T_e v_{te}$ respectively, the wavenumbers k_{\parallel} and k_{\perp} are normalised to L_n and ρ_e respectively, and frequencies are normalised by v_{te}/L_n . Combining equation 1 with the quasi-neutrality condition, a Boltzmann ion response ($k_{\perp}\rho_i \gg 1$) and Ampere's law gives the dispersion relation,

$$\frac{(\omega - \omega_*)^2}{1 + \tau} - (\omega - \omega_*)(\omega - \omega_D) - \omega_*\omega_D\eta_e + \frac{2(k_{\perp}k_{\parallel})^2}{\beta_e} = 0 \quad (2)$$

where $\beta_e = 8\pi n_0 T_e / B_0^2$, $\omega_D = 2L_n\omega_*/R = 2\epsilon_n\omega_*$ and $\tau = T_e/T_i$. When $\tau = 1$ the solution of the ballooning equation 2 is,

$$\frac{\omega}{\omega_*} = \frac{2}{3} \left[-(1 + \epsilon_n) \pm \sqrt{(1 + \epsilon_n)^2 - 3/2[2\epsilon_n(1 + \eta_e) + 1/2 - (2\epsilon_n/\alpha_e)]} \right] \quad (3)$$

and is unstable for,

$$\alpha_e > \frac{2\epsilon_n}{2\epsilon_n(1 + \eta_e) - (2/3)(1 + \epsilon_n)^2 + 1/2} \quad (4)$$

where $\alpha_e = q^2 R \beta_e / L_n$.

Using the gyrokinetic code GS2 [6] we test the validity of equation 3. Figure 1 shows the

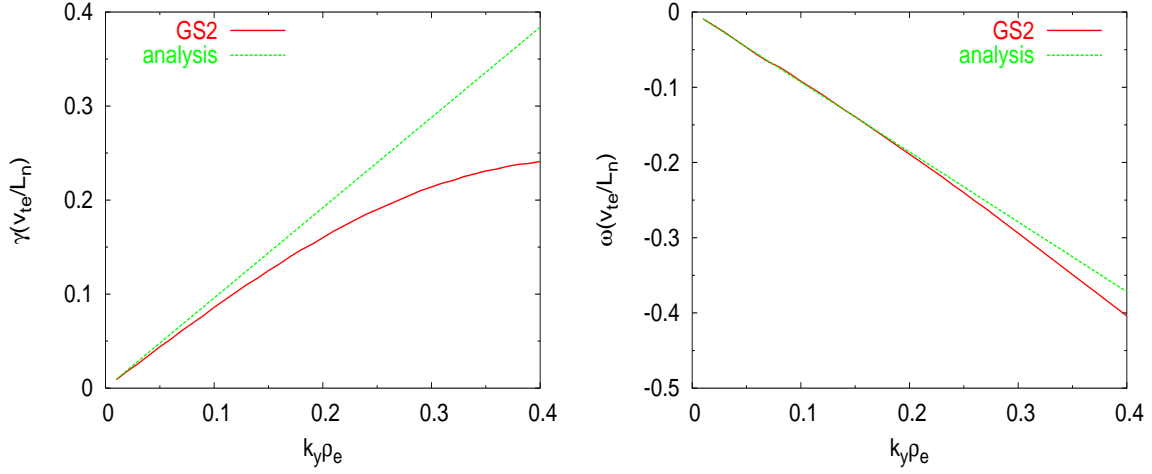


Figure 1: *ETG growth rates (left) and real frequencies (right) as a function of k_y calculated from equation 3 and using the gyrokinetic code GS2*

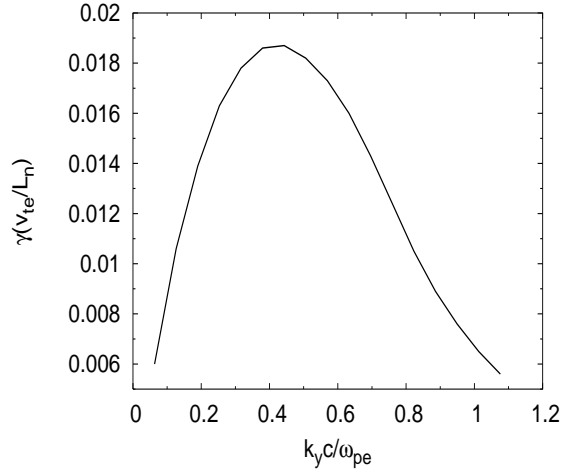


Figure 2: *Growth rate as a function of k_y (normalised to the skin-depth) for $\eta_e = 1$ and $\beta_e = 0.05$. The electrostatic ETG mode is stable*

ETG dispersion relation using equation 3 and GS2 calculations for the electromagnetic and electrostatic cases with $\epsilon = 0$, $\hat{s} = 0$, $\alpha = -q^2 R d\beta/dr = 0$, $\eta_e = 3$, $\beta_e = 0.02$, $q = 4$ and $\epsilon_n = 0.4$. The curvature and ∇B drifts have been set constant in GS2. Equation 3 is seen to be in good agreement with the code with in the limits of the analysis. The inclusion of full ion physics in the simulation has been tried and a Boltzmann ion response is appropriate.

Equation 4 predicts that the mode will be unstable for all values of η_e given a large enough value of α_e . Figure 2 shows unstable modes for $\eta_e = 1$ and $\beta_e = 0.05$ (all other parameters as above) with $k_{\perp} c / \omega_{pe} \lesssim 1$, which is below the critical η_e calculated from the ETG critical gradient formula of reference [8]. This could allow sub-critical turbulence to develop at ρ_e scales in tokamaks.

Preliminary nonlinear simulations using GS2 produce a large thermal transport

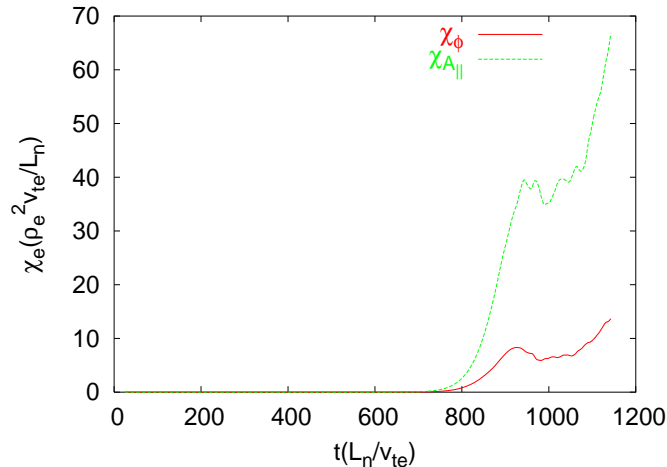


Figure 3: *Thermal transport coefficients vs. time produced by $\mathbf{E} \times \mathbf{B}$ advection χ_ϕ and magnetic flutter χ_{A_\parallel} . Flux-tube dimensions are $L_x = L_y = 628\rho_e$ and number of grid points are $n_x = 200$ and $n_y = 32$.*

coefficient, dominated by the magnetic nonlinearity (magnetic flutter). Figure 3 shows the thermal transport coefficients resulting from the $\mathbf{E} \times \mathbf{B}$, and A_\parallel nonlinearities for the regime shown in figure 2. Streamers are still observed in the electrostatic potential, while contours of A_\parallel appear isotropic (figure 4). The large transport shows not only the possibility of ETG thermal transport below the critical gradient calculated in [8], but also (since $\alpha = 0$ and $\hat{s} = 0$) in a region of \hat{s} - α space predicted to have low transport in [1, 2].

Further nonlinear simulations are required to determine the role of the electromagnetic ETG mode, in the saturation of a fully unstable ETG spectrum. Mixing length estimates based on the results of a gyrokinetic integral code [9] show the transport coefficient to peak at $ck_y/\omega_{pe} \sim 1$, giving a possible β scaling (figure 5). ETG turbulence simulations in the spherical tokamak MAST, show signatures that could be explained by this mode [10] i.e. transport peaks at $ck_y/\omega_{pe} \sim 1$, only modes with $ck_y/\omega_{pe} \lesssim 1$ have large A_\parallel perturbations (figure 6) relative to the amplitude of ϕ , a sensitivity to the transport on longer wavelengths was also noted (flutter transport was negligible).

3. Trapped Electrons

A strong reduction in ETG thermal transport with the removal of trapped electrons [7] in GS2 calculations is thought to be due to a reduction in the linear ETG growth rate (figure 7). Trapped particles are removed, by integrating the distribution function over all passing pitch angles, and neglecting trapped particle pitch angles. This differs from the conventional method of removing trapped particles by setting $\epsilon = r/R = 0$, in that finite ϵ effects on passing particles are retained, and the equilibrium density is reduced by a factor $1 - \sqrt{\epsilon}$ ($\sqrt{\epsilon}$ is the fraction of trapped particles present).

Figure 7 shows how the growth rates vary with ϵ , with out and with trapped electrons included, for the cyclone parameters $\epsilon_n = 0.45$, $\eta_e = 3.14$, $q = 1.4$, $\hat{s} = 0.8$, $\alpha = 0.45$,

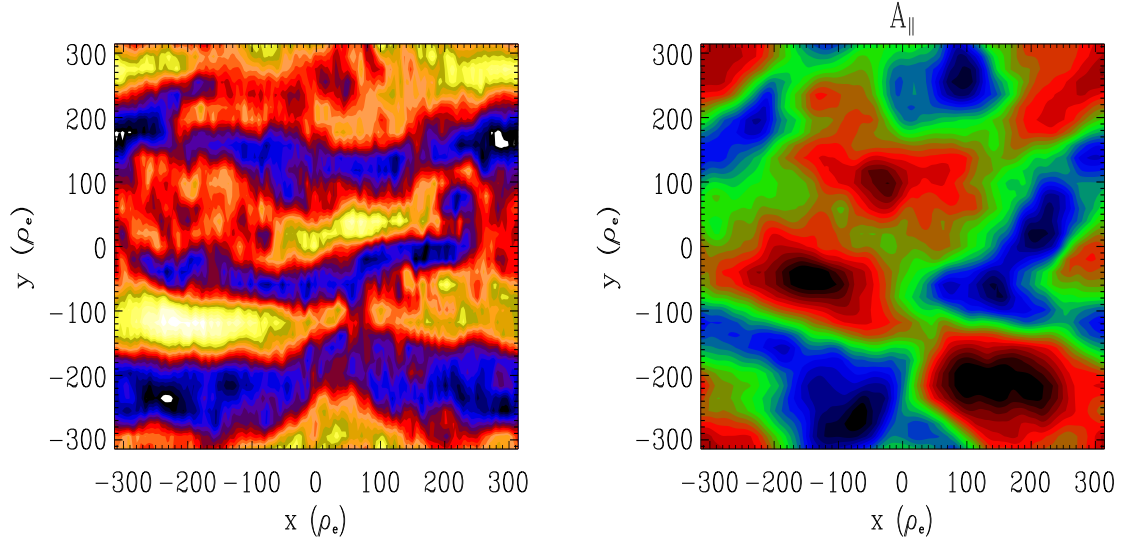


Figure 4: Snapshot of contours in the $x - y$ plane for ϕ (left) and A_{\parallel} (right)

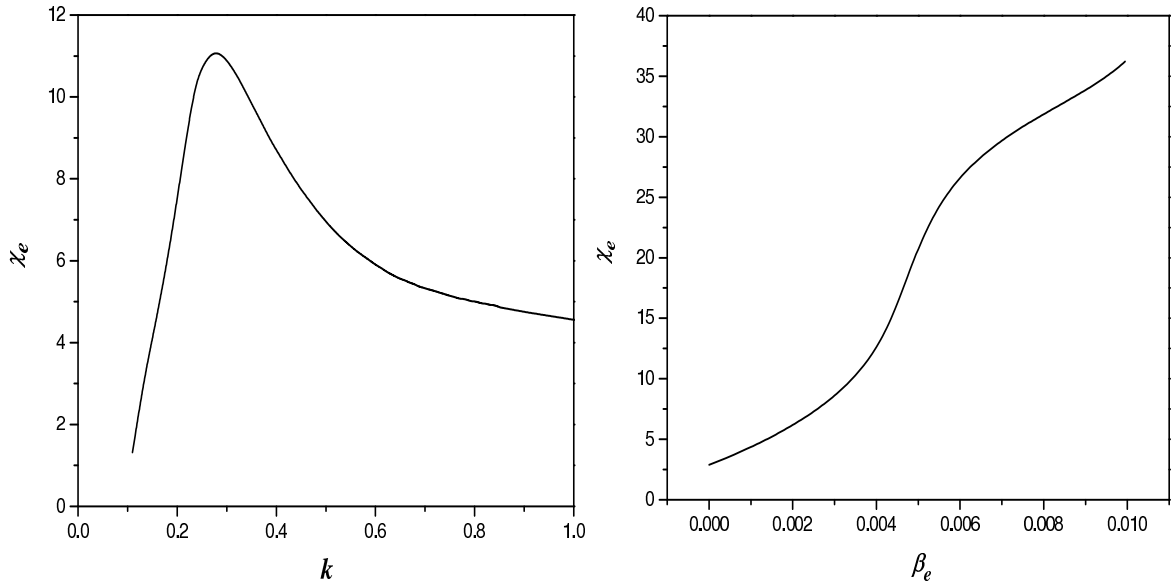


Figure 5: Mixing length estimate χ_e vs. $k = ck_y/\omega_{pe}$ (left) and vs. β_e maximised over k (right). Base parameters are $\epsilon_n = 0.3$, $\eta_e = 2$, $q = 2$, $\hat{s} = 1$, $\alpha = 0.4$, $\beta_e = 0.005$

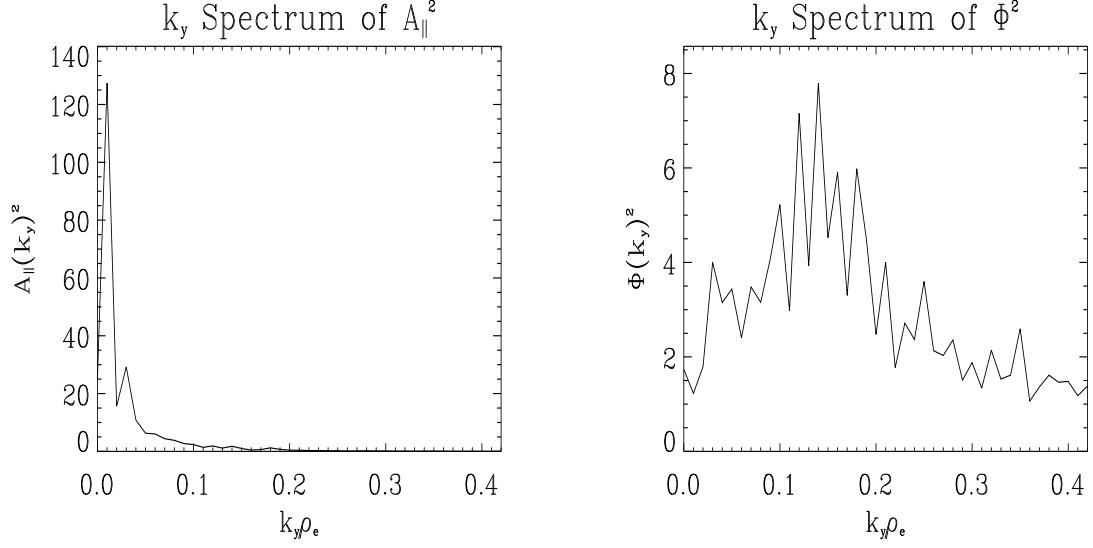


Figure 6: Snap shot of A_{\parallel} and ϕ spectra at the end of an ETG simulation in spherical tokamak geometry. Modes are summed over k_x .

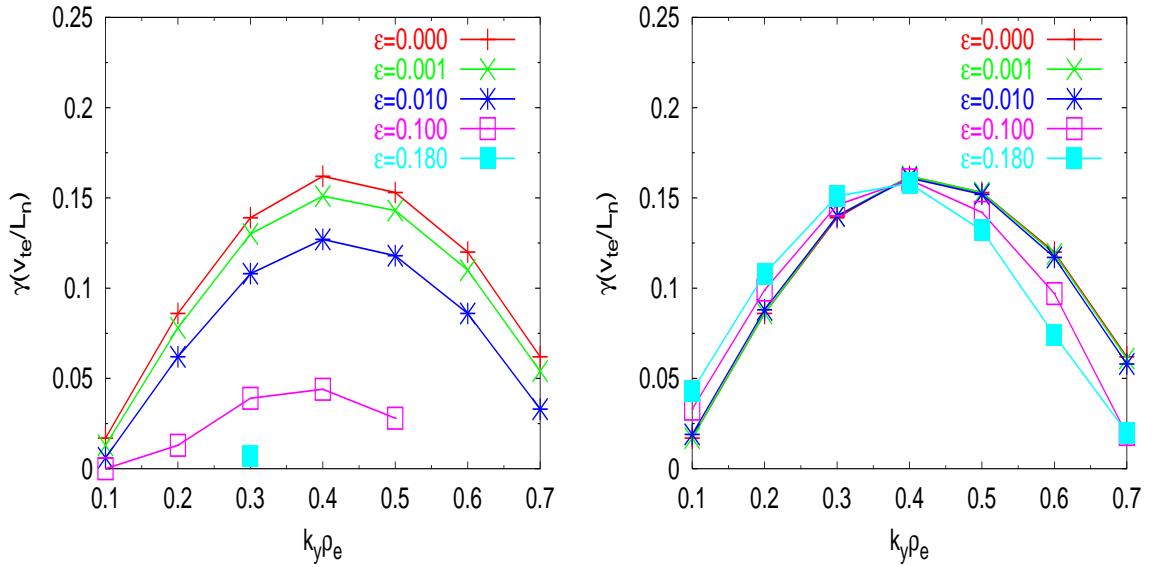


Figure 7: Variation of growth rate vs k_y for differing values of $\epsilon = r/R$, with out trapped particles (left) and with trapped particles (right) included in the pitch angle integration

$\beta_e = 0.013$. The growth rates are relatively insensitive to ϵ when trapped particles are included. This indicates that the ETG instability is largely contributed to by particles with large pitch angle, rather than the bounce motion of the trapped particles playing any significant role ($\omega \ll \omega_B$ therefore the trapped particles are effectively passing).

In future work it would be interesting to investigate whether thermal anisotropy in the equilibrium, which would change the pitch angle distribution, effects ITG and ETG growth and transport.

4. Conclusions

An electromagnetic ETG mode exists on the scale $ck_{\perp}/\omega_p \lesssim 1$, with strong ballooning character. Analysis and simulation predict that this mode can be unstable below the ETG critical gradient, for large enough β . Under such a regime, the transport produced by the mode may be of significance to experiments, based on mixing length estimates and preliminary nonlinear simulation. It is not clear at present what role this mode will play in the saturation of streamers for a fully unstable ETG spectrum. However it does illustrate the importance of including longer wavelengths in electromagnetic ETG turbulence simulations where this mode is unstable. This makes the already computationally challenging task of resolving to sub- ρ_e scales even more difficult in such simulations.

Neglecting large (trapped) pitch angles in linear and nonlinear ETG calculations, causes a reduction in the linear growth rate and thermal transport. This is due to a hole in the distribution function, rather than the properties of trapped particles. The role of particles with these pitch angles may be of importance where there is thermal anisotropy in the equilibrium.

The authors would like to thank Bill Dorland for useful discussions. GS2 simulations were performed on the WestGrid computing resources, which are funded in part by the Canada Foundation for Innovation, Alberta Innovation and Science, BC Advanced Education and the participating research institutions. Financial support has been provided by NSERC Canada and by the Canada Research Chair Program.

References

- [1] W. Dorland, F. Jenko, M. Kotschenreuther, and B. N. Rogers. Electron temperature gradient turbulence. *Physical Review Letters*, 85(26):5579, 2000.
- [2] F. Jenko, W. Dorland, M. Kotschenreuther, and B. N. Rogers. Electron temperature gradient driven turbulence. *Physics of Plasmas*, 7(5):1904, 2000.
- [3] F. Jenko and W. Dorland. Nonlinear electromagnetic gyrokinetic simulations of tokamak plasmas. *Plasma Physics and controlled Fusion*, 43:A141, 2001.
- [4] N. Joiner. *Microinstabilities in spherical tokamaks*. PhD thesis, Imperial College London, 2005.
- [5] J. Y. Kim and W. Horton. Electromagnetic effect on the toroidal electron temperature gradient mode. *Physics of Fluids*, B3(11):3194, 1991.

- [6] M. Kotschenreuther, G. W. Rewoldt, and W. M. Tang. Comparison of initial value and eigenvalue codes for kinetic toroidal plasma instabilities. *Computer Physics Communications*, 88:128, 1995.
- [7] N. Joiner and A. Hirose. Proceedings of 33rd EPS conference on plasma physics. Rome, 2006. paper P1.198.
- [8] F. Jenko, W. Dorland, and G. W. Hammett. Critical gradient formula for toroidal electron temperature gradient modes. *Physics of Plasmas*, 8(9):4096, 2001.
- [9] A. Hirose and M. Elia. Finite β destabilization of skin sized drift modes in tokamaks. *Physica Scripta*, 65(3):257, 2002.
- [10] N. Joiner, D. Applegate, S. C. Cowley, W. Dorland, and C. M. Roach. Electron temperature gradient driven transport in a MAST H-mode plasma. *Plasma Physics and Controlled Fusion*, 48(5):685, 2006.